High-Pressure Study of *h.c.p.*-Argon

J. Wittlinger,* R. Fischer, S. Werner, J. Schneider and H. Schulz

Institut für Kristallographie und Angewandte Mineralogie der Universität München, Theresienstrasse 41, 80333 München, Germany. E-mail: wittlinger@lrz.uni-muenchen.de

Abstract

Argon, used as pressure medium in high-pressure experiments, crystallizes in a hexagonal close-packed structure when the argon is loaded cryogenically in the diamond anvil cell. The behaviour under pressure reveals elastic properties comparable to that of *f.c.c.*-argon (*f.c.c.* = face-centred cubic). The bulk modulus is 6.5 (1.3) GPa. The initially good quality of the individual crystals suffers strongly under pressure increase. Heating the cell to 393 K at 8.5 GPa recreates the crystal structure, accompanied by a pressure decrease of more than 1 GPa.

1. Introduction

1.1. *Inert gases under pressure*

Argon under pressure has already been investigated up to a pressure of 80.6 GPa (Finger, Hazen, Zou, Mao & Bell, 1981; Ross, Mao, Bell & Xu, 1986). Both papers report an *f.c.c.* structure with a very high compressibility, which stays inert under pressure. In low-temperature experiments metastable *h.c.p.* phases of argon have been observed, which seem to become stable when impurities such as oxygen or nitrogen are added to the gas (Meyer, Barrett & Haasen, 1964). This modification was mainly observed near the melting point. The argon–nitrogen phase diagram shows a region of an Ar–N_2–*h.c.p.* structure in the region directly below the liquid phase, which, however, seems to disappear at 0% nitrogen (Barett & Meyer, 1964, 1965). Theoretical calculations of the high-pressure behaviour of argon show nearly equivalent energy levels for the *f.c.c.* and *h.c.p.* modifications in the low-pressure range. Only in megabar regions is there a preference for the *h.c.p.* configuration (McMahan, 1986). Different groups have extensively investigated other inert gases in high-pressure experiments, but only helium and xenon show a *h.c.p.* structure under certain conditions (Loubeyre *et al.*, 1993; Jephcoat *et al.*, 1987), the other inert gases show *f.c.c.* structures (*e.g.* for krypton: Polian, Besson, Grimsditch & Grosshans, 1989; for neon: Hemley *et al.*, 1989).

1.2. *Ar as high-pressure medium*

In recent years argon plays a more and more important role in high-pressure crystallography as a pressure medium, due to its physical properties. Results of X-ray experiments can be affected by modulations in the background, originating from diffracting material in the beam path such as beryllium, steel and diamonds, and also from the pressure medium. Especially in the case of signals originating from small samples, non-ideal crystals and amorphous or partially amorphous phases, the intensities are comparable to the background. In such cases it is often hard to distinguish between the background signal and the sample signal. Therefore, the knowledge of the structure of the background radiation turns out to be of crucial importance for the extraction of correct intensity values from the raw data.

2. Experimental

2.1. *Preparation of the diamond anvil cell*

All experiments were carried out with diamond anvil cells, suitable for angle-dispersive high-pressure experiments (Werner, Kim-Zajonz, Wittlinger & Schulz, 1996). The argon was loaded cryogenically. Hereby, the cell, equipped with some pieces of ruby in the sample chamber, is placed in a box which is cooled with liquid nitrogen from the outside. Then, liquid argon is dropped in the box. The argon remains in the liquid state at the boiling point of nitrogen, so the cell can be drowned completely in the argon (boiling temperatures: $T_{Ar} = 87$ K, $T_{N_2} = 77$ K). In argon only weak convection arises. This is an important prerequisite to prevent single crystals, such as ruby, from being washed from the diamond culets. The cell can be closed and subsequently heated up to room temperature. For all experiments commercial welding argon was used, which shows a purity better than 99.996% (DIN 32 526). If the initial pressure exceeds 1.2 GPa, the argon is already solid when it is heated up. If it is below 1.2 GPa, the argon crystallizes at room temperature by a further pressure increase. The pieces of ruby in the cell are used for pressure measurement

and as an internal standard in powder diffraction experiments at the same time.

2.2. Data collection

As the argon is polycrystalline, the usual single crystal methods are difficult to perform. On the other hand, because of the small amount of individual crystals (*ca* 5–15 pieces) in the cell, powder methods suffer strongly from preferred orientation effects.

2.2.1. *CAD-4 measurements.* Orientations of single crystals of argon were determined on a CAD-4 four-circle diffractometer at two different pressures using $Mo\,K\alpha$ radiation, originating from a sealed tube in combination with a graphite monochromator. As there are always several single crystals in the cell this is a very inconvenient method to determine the lattice constants of the argon matrix, but in this way some information about the individual crystals could be obtained. Problems mainly arise because of the low intensity of the individual reflections and because of the difficulty in selecting several reflections of one single crystal to obtain its orientation.

2.2.2. *Powder diffraction measurements.* Another approach was to use a newly developed cell holder on a focusing powder diffractometer (Stoe Stadi-P). The setup allows a continuous rotation of the diamond anvil cell around its symmetry axis, which in turn is set parallel to the primary beam (Wittlinger, 1997). An additional oscillatory movement of the cell about an axis vertical to the diffraction plane ($\Delta\omega = \pm 10°$) may be turned on (for settings of diffraction angles throughout the paper, see, *e.g.* Giacovazzo, 1992). In such a way, an optimum of the possible randomization of crystallite orientations is reached. With this setup powder patterns suitable for Rietveld refinement may be obtained. Using $Mo\,K\alpha_1$ radiation (55 kV, 30 mA) and a linear position detector (500 channels of $2\theta = 0.02°$), 1–2 d data collection time is needed per diagram. The insertion of several ruby crystallites with different orientations into the cell, together with the rotation and oscillation of the cell itself, produces a corundum powder diagram of sufficient quality to be refined as a second phase in a multiple-phase Rietveld refinement (Fig. 1). As a third phase. Fe can be introduced, to model the gasket signals. All refinements were carried out using $WYRIET3.0.$ (Schneider & Dinnebier, 1991). Additional powder
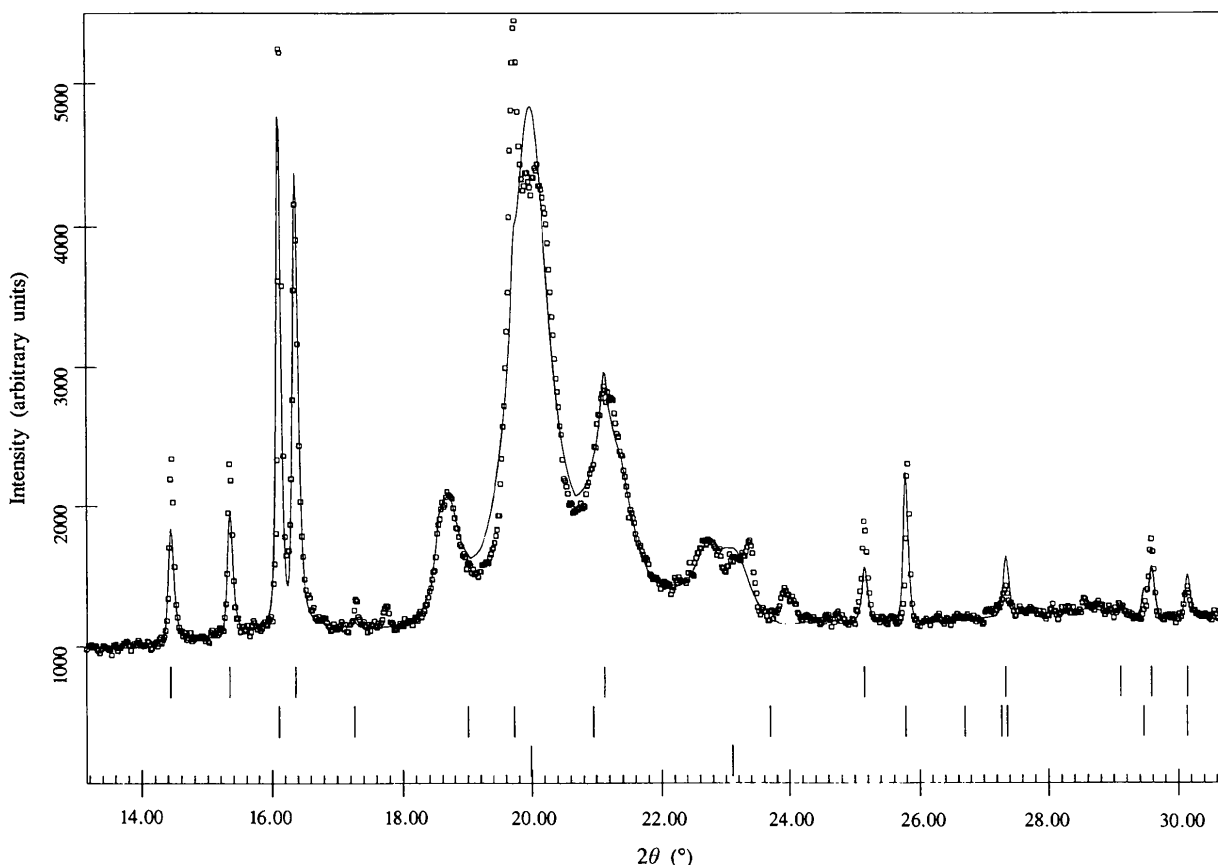

Fig. 1. Multiple Rietveld refinement of a typical powder pattern at 6.5 GPa after annealing the cell ($R_{wp} = 7.5$). The vertical bars designate the line positions of the Ar, Al_2O_3 and Fe phases, respectively. Ar and Al_2O_3 are the contents of the sample chamber, while Fe signals originate from the gasket. Unidentified lines are due to additional material in the beampath such as beryllium and diamonds.

diffraction lines arise, due to diamond, beryllium and different phases of iron from the gasket. These lines are ignored in the refinement process, because it seems to be impossible to find a suitable model for these signals.

2.2.3. *Image plate measurements.* In addition, detecting the argon on image plates proved to be very useful, because it seems to be the best way to obtain information on the number of crystals under consideration and their quality and mosaicity. These images are obtained within a few hours on a CAD-4 diffractometer with a special setup to fix the plate in a determined position and distance. The cell is rotated around φ at $\omega = 0°$ and $\kappa = 0°$. The images can be stored digitally and so it is possible to derive information by means of suitable software, *e.g. d* spacings, χ width of individual reflections *etc.* The argon reflections can also be interpreted as spotty powder rings, which can be integrated angularly (Hammersley, 1987), to obtain conventional spectra as input, *e.g.*, for Rietveld refinement programs. Here, the image plates only were used for visualization of the crystallites in the cell.

3. Results and discussion

3.1. *Structure*

Obviously, argon here is not always in the *f.c.c.* modification, as reported from other high-pressure experiments. By using the cryogenically loading procedure, however, also a *h.c.p.* modification can be obtained (space group: $P6_3/mmc$). If a pressure above 1.2 GPa is reached under liquid argon conditions, and the cell is heated up subsequently, the *h.c.p.* modification crystallizes in the cell. However, if the pressure is

below 1.2 GPa when the cell is heated up and the pressure is increased above the solidus at room temperature, the *f.c.c.* modification is found (Fig. 2). In all other investigations on argon under pressure a gas loader was used to close the cell. Therefore, the argon always crystallizes at ambient temperature conditions. It can be stated that if the gas crystallizes under pressure at around 80 K, the argon has the *h.c.p.* modification, but if it crystallizes at room temperature, it has the *f.c.c.* modification. Comparison with results of calculations shows that both modifications seem to have almost the same formation energies in the pressure range in which the crystallization process takes place (McMahan, 1986). Thus, a difference in thermodynamic conditions, *e.g.* a different temperature, can easily favour one or the other structure.

3.2. *Equation of state*

The pressure dependence of the *h.c.p.* lattice constants obtained can be described with a Birch–Murnaghan equation of state. The best approach here seems to fix K' at 4, because of the small pressure range of the measurements. As the volume at ambient pressure cannot be an experimental result, it must be considered as an additional fitting parameter and so the bulk modulus K and the initial volume V_0 are fitted to the data, using function (1), where p denotes the pressure and V the corresponding volume of the unit cell (Fig. 3)

$$p = 3/2K[(V_0/V)^{7/3} - (V_0/V)^{5/3}]. \qquad (1)$$
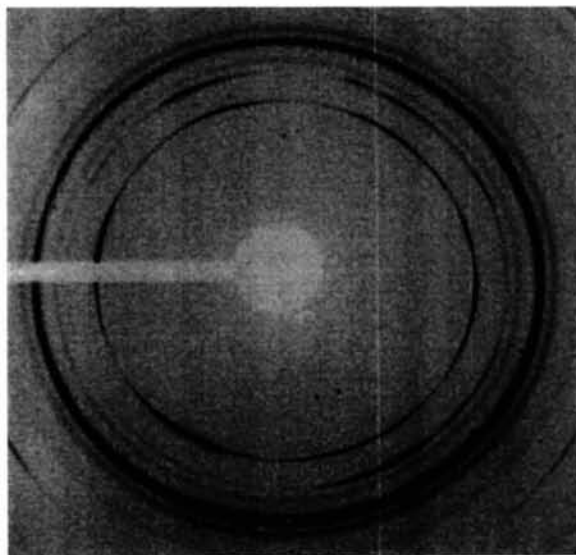

Fig. 2. Image plate of a pressure cell with *f.c.c.*-argon at 9 GPa. The signals originating from the argon crystals here are smeared out ring segments of ~40° in χ.
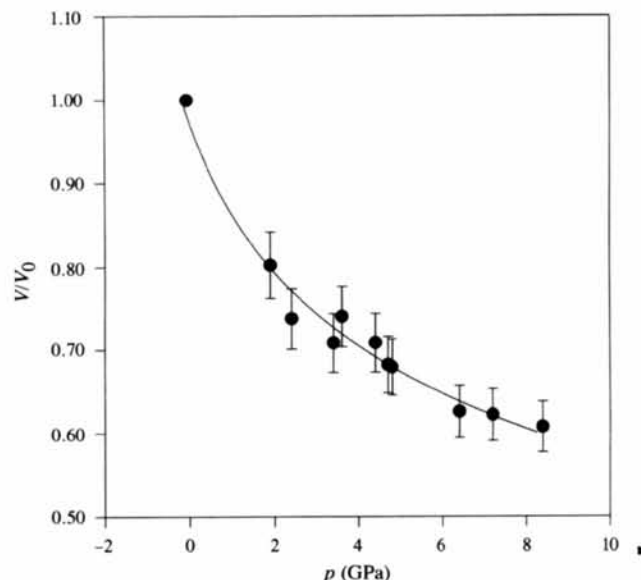

Fig. 3. Relative volume change *versus* pressure of *h.c.p.*-argon. The line is a fitted Birch–Murnaghan equation of state of first order. The volume at ambient pressure is an additional fitting parameter with the value $V_0 = 78\,(3)\,\text{Å}^3$.

The fitted values are $K = 6.5\,(1.3)$ GPa for the bulk modulus and $V_0 = 78\,(3)\,\text{Å}^3$ for the ambient pressure volume, which leads to a corresponding bond length of $a = 3.8\,(3)\,\text{Å}$ (Fig. 3). The calculated lattice constants are $a = 3.8\,(3)$ and $c = 6.2\,(5)\,\text{Å}$. The results agree with those obtained for *f.c.c.*-argon, namely: $K = 7.2\,(2)$ GPa and $a = 4.0\,(2)\,\text{Å}$ (derived from Ross, Mao, Bell & Xu, 1986). The c/a ratio of the unit cell stays at the ideal value of 1.633 within the experimental errors in the whole pressure range investigated, despite the obvious macroscopic shear deformation of the crystals (see below).

3.3. Modification

Image plate measurements show a polycrystalline substance (*ca* 5–15 crystals in the cell, depending on the individual high-pressure run), with initially sharp single crystal reflections. CAD-4 measurements show that at low pressures, up to 3 GPa, the angular width of the argon reflections is comparable to that of ruby reflections, indicating individual crystals of good quality and unexpected small mosaicity. Also the imaging plate measurements at these pressures show the argon reflections as round spots. A subsequent pressure increase shows a substantial broadening of the reflections in χ. Around 10 GPa, it is common that the broadening in χ and ω is around 10–20° for both the *f.c.c.* and the *h.c.p.* modifications. This is in contrast to the earlier observations (Finger, Hazen, Zou, Mao & Bell, 1981), where a recrystallization of the argon at every pressure value and no decrease in quality of the single crystals was reported.

In addition, also in θ a broadening of the reflections or lines can be observed. In the powder diffraction patterns, the reflection widths are broadened by a factor of ~ 5 at 8.5 GPa compared with the initial value at

1.6 GPa (Fig. 4). The line broadening has a strong (*hkl*) dependence. The (100) line shows about half of the width of the (011) line. The single crystals seem to be deformed following the changing shape of the sample chamber at different pressure values. Thus, the argon matrix might show a pressure gradient, increasing with pressure. The line width in θ indicates, *e.g.* at 8.5 GPa, a gradient of ~ 0.2 GPa.

Above 9 GPa argon becomes a substance which seems to be rather a textured powder specimen than a single crystal (Fig. 2). This effect can be completely reversed by heating the whole cell to 393 K for several hours. The reflections in the powder pattern become as sharp as the initial ones and the crystallinity of the argon is recreated. So, the pressure gradient obviously disappears and the tension in the argon, probably responsible for the broadening in χ, vanishes. Obviously, the slight temperature increase gives the Ar atoms enough mobility to recreate the crystal structure completely. This treatment was accompanied by a pressure decrease of more than 1 GPa, which can be explained at first as a mechanical destabilization of the pressure cell and second as a volume decrease in the argon matrix, caused by the restructuring. The pressure decrease corresponds to a volume decrease of argon by $\sim 3\%$, which may be caused by repackaging the squeezed argon in an ideal structure.

The results confirm the non-hydrostaticity of the argon matrix and its development under pressure, which was already mentioned (Bell & Mao, 1981). Obviously there is a strong influence on the macroscopic structure of the sample under consideration and the quality of single crystals depends strongly on hydrostatic conditions in the cell. It is, however, not allowed to assume automatically an effect on the microscopic structure under consideration. Despite the strong squeezing of the crystals along the symmetry axis of the cell, no effect on the c/a ratio could be observed. Effects of the non-hydrostaticity of the pressure medium argon on high-pressure experiments can be avoided by heating the sample chamber to ~ 373 K after every step of pressure increase. As the heating of the gasket implies problems of mechanical stability in ultra-high-pressure experiments, the heating with an appropriate laser, focused on the sample chamber, could be a great improvement in high-pressure work with single crystals, as it is already common use in powder diffraction experiments.
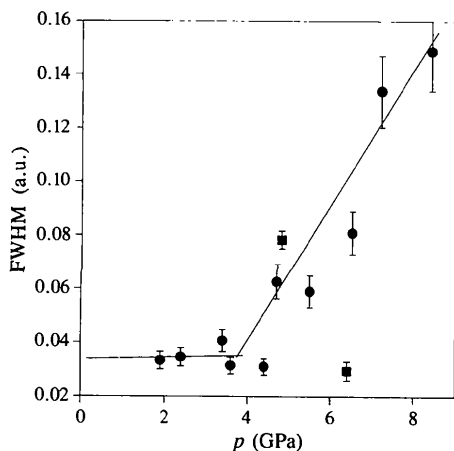

Fig. 4. Pressure dependence of the line width of the (011) line. Between 4 and 5 GPa, line broadening, originating from directed pressure application on the argon crystals, sets in. The lines serve as a guide to the eye.

References

Barrett, C. S. & Meyer, L. (1964). *J. Chem. Phys.* **41**, 1078–1081.

Barrett, C. S. & Meyer, L. (1965). *J. Chem. Phys.* **42**, 107–112.

Bell, M. P. & Mao, H. K. (1981). *Carnegie Inst. Washington Yearb.* **80**, 404–406.

Finger, L. W., Hazen, R. M., Zou, G., Mao, H. K. & Bell, M. P. (1981). *Appl. Phys. Lett.* **39**, 892–894.

Giacovazzo, C. (1992). Editor. *Fundamentals of Crystallography*. Oxford University Press.

Hammersley, A. P. (1987). *FIT2D*. 1987–1995. European Synchrotron Radiation Facility, Experimental Division Programming Group.

Hemley, R. J., Zha, C. S., Jephcoat, A. P., Mao, H. K., Finger, L. W. & Cox, D. E. (1989). *Phys. Rev. B*, **39**, 11820–11826.

Jephcoat, A. P., Finger, L. W., Mao, H. K., Cox, D. E., Hemley, R. J. & Zha, C. S. (1987). *Phys. Rev. Lett.* **59**, 2670–2672.

Loubeyre, P., LeToullec, R., Pinceaux, J. P., Mao, H. K., Hu, J. & Hemley, R. J. (1993). *Phys. Rev. Lett.* **71**, 2272–2275.

McMahan, A. K. (1986). *Phys. Rev. B*, **33**, 5344–5349.

Meyer, L., Barrett, C. S. & Haasen, P. (1964). *J. Chem. Phys.* **40**, 2744–2745.

Polian, A., Besson, J. M., Grimsditch, M. & Grosshans, W. A. (1989). *Phys. Rev. B*, **39**, 1332–1336.

Ross, M., Mao, H. K., Bell, M. P. & Xu, J. A. (1986). *J. Chem. Phys.* **85**, 1028–1033.

Schneider, J. & Dinnebier, R. (1991). *Mater. Sci. Forum*, **277**, 79–82.

Werner, S., Kim-Zajonz, J., Wittlinger, J. & Schulz, H. (1996). *Proceedings of the Workshop on the Use of Ultrashort Wavelengths*, pp. 26–29. Hamburg, Germany: Hasylab.

Wittlinger, J. (1997). Thesis at the Institut für Kristallographie und Mineralogie der Universität München.